NJC

Accepted Manuscript

This is an *Accepted Manuscript*, which has been through the Royal Society of Chemistry peer review process and has been accepted for publication.

Accepted Manuscripts are published online shortly after acceptance, before technical editing, formatting and proof reading. Using this free service, authors can make their results available to the community, in citable form, before we publish the edited article. We will replace this *Accepted Manuscript* with the edited and formatted *Advance Article* as soon as it is available.

You can find more information about *Accepted Manuscripts* in the Information for Authors.

Please note that technical editing may introduce minor changes to the text and/or graphics, which may alter content. The journal's standard Terms & Conditions and the Ethical guidelines still apply. In no event shall the Royal Society of Chemistry be held responsible for any errors or omissions in this *Accepted Manuscript* or any consequences arising from the use of any information it contains.

ROYAL SOCIETY OF CHEMISTRY

www.rsc.org/njc

Cite this: DOI: 10.1039/c0xx00000x

www.rsc.org/xxxxxx

ARTICLE TYPE

Tuning the nuclearity of iron(III) polynuclear clusters by using tetradentate Schiff-base ligands

Alexandre Abhervé,[a] Juan Modesto Clemente-Juan,[a] Miguel Clemente-León,*[a] Eugenio Coronado,*[a] Jaursup Boonmak[b] and Sujittra Youngme[b]

Received (in XXX, XXX) Xth XXXXXXXXX 20XX, Accepted Xth XXXXXXXXX 20XX
DOI: 10.1039/b000000x

Three novel octanuclear, hexanuclear and tetranuclear complexes of high-spin Fe(III) ions were obtained by the reaction of *N,N'*-Bis-(1R-imidazol-4-ylmethylene)-ethane-1,2-diamine ligand (R= H, CH_3) and its derivatives with $Fe(ClO_4)_3{\cdot}6H_2O$ and KSCN. The tetradentate Schiff-base ligand acts as bis(bidentate) chelating bridge between two adjacent high-spin Fe(III) centers. The presence of a methyl group in the imidazolyl substituent, the change of counterion or the replacement of imidazole by pyridine has a drastic effect in the nuclearity of the cluster. The magnetic properties of all compounds exhibit antiferromagnetic interactions *via* μ-oxo or μ-hydroxo pathways in Fe(III) dimers.

Introduction

Self-assembly processes between organic ligands and metal ions may lead to the formation of functional supramolecular architectures exhibiting unusual properties[1,2] or interesting host−guest behaviors.[3] Imidazole and imidazolyl-containing ligands have been widely used in coordination chemistry due to their versatility in the preparation of polynuclear complexes, which are of interest in magnetochemistry, and in connection with the design of model compounds mimicking the core structures of active sites of some metalloproteins.[4] More recently, the use of flexible imidazole ligands have afforded the preparation of many coordination complexes with interesting topologies and functional properties such as ferroelectricity,[5] porosity, fluorescence[6] and chemisorption-induced magnetic properties.[7]

One of the most used strategies for the incorporation of imidazolyl moiety in ligands is the condensation of a diamine with an imidazolecarboxyaldehyde.[4] Tridentate,[8] tetradentate[9,10] and hexadentate[11] Schiff base ligands have been prepared with this strategy. Reactions of these ligands with iron(II) have afforded many examples of mononuclear spin-crossover complexes. In the case of tetradentate imidazolyl ligands, mononuclear neutral ferrous complexes of formula $[FeL(NCS)_2]$ have been reported.[10]

The reaction of iron(III) with imidazolyl Schiff-base tetradentate ligands has been little explored. The preparation of high nuclearity species are often encountered in iron(III) chemistry due to the high charge-to-size ratio of iron(III) ion and the resulting propensity to form oxo bridges.[12] Polynuclear iron complexes raise interest as magnetic materials, such as single-molecule magnets (SMM),[13] but also due to their biological importance.[14]

Herein, we report that reaction of iron(III) with *N,N'*-Bis-(1R-imidazol-4-ylmethylene)-ethane-1,2-diamine and its derivatives (L_1 and L_2, Scheme 1), and NCS^- permit the preparation of a family of Fe(III) ring cationic clusters. They are formed by Fe^{III}-O-Fe^{III} dimers bridged by the imidazolyl ligand in a bis(bidentate) mode. The number of Fe^{III}-O-Fe^{III} dimers of the cluster (four or three) and, therefore, its nuclearity (octanuclear or hexanuclear) can be controlled by changing the counterion or introducing a bulky substituent in the ligand. Furthermore, the related tetradentate pyridine ligand, L_3 (Scheme 1) leads to a tetranuclear neutral cluster. The magnetic properties of the three clusters are reported and discussed.

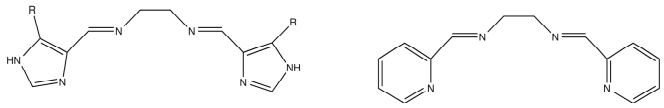

R = H (L_1), CH_3 (L_2) L_3

Scheme 1. Molecular structure of the ligands used in this work.

Experimental section

Syntheses

N,N'-Bis-(1-H-imidazol-4-ylmethylene)-ethane-1,2-diamine (L_1) was prepared by the reaction of 4-imidazolecarboxaldehyde (961 mg, 10.00 mmol) and ethylenediamine (334 μL, 5.00 mmol) in acetonitrile (100 mL) for 45 min at 353 K. *N,N'*-Bis-(1-CH_3-imidazol-4-ylmethylene)-ethane-1,2-diamine (L_2)[15] and N,N'-Bis-(pyridin-2-ylmethylene)-ethane-1,2-diamine (L_3) were prepared according to the literature method.[16] All other chemicals are commercially available and were used as received without further purification.

$[Fe_8(\mu\text{-}L_1)_8(\mu\text{-}O)_4(NCS)_8](ClO_4)_5(NCS)_3(H_2O)_6$ (1). KSCN (195 mg, 2 mmol) was added to a methanolic solution (20 mL) of

$Fe(ClO_4)_3 \cdot 6H_2O$ (354 mg, 1 mmol). The solution was filtered and a solution of L_1 (216 mg, 1.00 mmol) in methanol (30 mL) was added to the filtrate. The mixture was stirred for 30 min at room temperature. The colour of the mixture turned orange. Orange crystals of **1** suitable for X-ray crystal analysis were obtained by slow diffusion of diethyl ether into this solution. Anal. Calc. for $C_{91}H_{108}Cl_5Fe_8N_{59}O_{30}S_{11}$: C, 31.4; H, 3.1; N, 23.7; S, 10.1. Found: C, 31.7; H, 3.2; N, 22.9; S, 9.9 %. IR (selected peaks): 2051 (NCS), 1629 (imine) and 1090 (ClO_4^-) cm^{-1}.

$[Fe_6(\mu\text{-}L_2)_6(\mu\text{-}O)_3(NCS)_6](ClO_4)_2(NCS)_4(CH_3CH_2OCH_2CH_3)_{0.5}(H_2O)_{3.5}(CH_3OH)_{2.5}$ (2). Compound **2** was synthesized in a similar manner to that of compound **1** by using ligand L_2 (244 mg, 1 mmol) instead of L_1. Anal. Calc. for $C_{86.5}H_{118}Cl_2Fe_6N_{46}O_{17.5}S_{10}$: C, 37.0; H, 4.2; N, 22.9; S, 11.4. Found: C, 35.5; H, 3.8; N, 21.9; S, 10.9 %. IR (selected peaks): 2050 (NCS), 1629 (imine) and 1121 (ClO_4^-) cm^{-1}.

$[Fe_4(\mu\text{-}L_3)_2(\mu\text{-}OH)_2(\mu\text{-}OHO)(NCS)_7(OH_2)](H_2O)_2(CH_3CN)_{0.5}$ (3). Compound **3** was synthesized in a similar manner to that of compound **1** by using ligand L_3 (238 mg, 1 mmol) instead. The mixture was stirred for 1h at room temperature. The color solution turned to dark purple and then a brown solid was formed. The precipitate was filtered and recrystallized in acetonitrile. The solution was allowed to stand undisturbed at room temperature. After three days, red prismatic crystals of **3** were obtained. Anal. Calc. for $C_{36}H_{38.5}Fe_4N_{15.5}O_{7.7}S_7$: C, 34.3; H, 3.1; N, 17.2; S, 17.7. Found: C, 35.0; H, 3.1; N, 17.3; S, 18.2 %. IR (selected peaks): 2030 (NCS), 1637 (imine) and 1400 ($\nu_{C=C}$) cm^{-1}.

$[Fe_6(\mu\text{-}L_1)_6(\mu\text{-}O)_3(NCS)_6](NO_3)_6(CH_3OH)_3(H_2O)$ (4). KSCN (195 mg, 2.00 mmol) was added to a solution of $Fe(NO_3)_3 \cdot 6H_2O$ (404 mg, 1.00 mmol) in methanol (20 mL). The solution was filtered and a solution of L_1 (216 mg, 1.00 mmol) in methanol (30 mL) was added to the filtrate. The mixture was stirred for 1h at room temperature. The color of the mixture turned orange. Orange crystals of **4** suitable for X-ray crystal analysis were obtained by diffusion of diethyl ether into the filtrate. The small amount of sample available prevented elemental analysis and powder X-ray diffraction measurements. IR (selected peaks): 2056 (NCS), 1632 (imine) and 1384 (NO_3^-) cm^{-1}.

$[Fe_6(\mu\text{-}L_2)_6(\mu\text{-}O)_3(NCS)_6](FeF_6)_{0.5}(NCS)_{4.5}(CH_3OH)_2$_(solvate) (5). KSCN (195 mg, 2.00 mmol) was added to a solution of $Fe(BF_4)_2 \cdot 6H_2O$ (338 mg, 1.00 mmol) in methanol (20 mL). Then a solution of L_2 (244 mg, 1.00 mmol) in methanol (30 mL) was added. The mixture was stirred for 1h at room temperature. The colour of the mixture turned orange. Orange crystals of **5** suitable for X-ray crystal analysis were obtained by diffusion of diethyl ether into the filtrate. Anal. Calc. for $C_{93.5}H_{142}F_3Fe_{6.5}N_{46.5}O_{15}S_{10.5}$: C, 38.5; H, 4.9; N, 22.4; S, 11.5. Found: C, 36.4; H, 3.2; N, 23.2; S, 11.8 %. IR (selected peaks): 2049 (NCS), 1629 (imine) and 482 (FeF_6^{3-}) cm^{-1}.

X-Ray crystallography

Single crystals of compounds **1-5** were mounted on glass fibres using a viscous hydrocarbon oil to coat the crystal and then transferred directly to the cold nitrogen stream for data collection. All reflection data were collected at 120 K on a Supernova diffractometer equipped with a graphite-monochromated Enhance (Mo) X-ray Source (λ = 0.71073 Å). The CrysAlisPro program, Oxford Diffraction Ltd., was used for unit cell determinations and data reduction. Empirical absorption correction was performed using spherical harmonics, implemented in the SCALE3 ABSPACK scaling algorithm. Crystal structures were solved by direct methods with the SIR97 program,[17] and refined against all F^2 values with the SHELXL-2013 program,[18] using the WinGX graphical user interface.[19a] All non-hydrogen atoms were refined anisotropically, and hydrogen atoms were placed in calculated positions and refined isotropically with a riding model. The details of data collection and structure refinements are provided in Table 1.‡ In compounds **1** and **5,** the presence of disordered thiocyanate and solvent molecules gave rise to a very weak scattering. Initial refinements revealed the presence of substantial volume of unresolvable solvent (CH_3OH and H_2O) molecules in **5**. The subroutine SQUEEZE from PLATON[19b] was used to remove the diffracting component of disordered solvents resulting in two voids of ca. 4163 $Å^3$ and 675 electrons/cell plus eight smaller voids of less than 25 $Å^3$ and 5 electrons/cell omitted. This corresponds to ca. 9 CH_3OH + 1 H_2O molecules per asymmetric unit. In compound **3**, one thiocyanate anion coordinated to Fe3 is disordered over two sites and has been modelled with an occupancy of 70:30 ratio.

0.5 mm glass capillaries were filled with polycrystalline samples of **2** and **3** and mounted and aligned on a Empyrean PANalytical powder diffractometer, using CuKα radiation (λ = 1.54177 Å). A total of 2 scans were collected at room temperature in the 2θ range 5-30°.

Physical measurements

C, H, N and S elemental analyses were measured on a CE Instruments EA 1110 CHNS Elemental analyzer. The Fe:S and Fe:S:Cl ratios were measured on a Philips ESEM X230 scanning electron microscope equipped with an EDAX DX-4 microsonde. Infrared spectra were recorded in the solid state (KBr pellets) on a Nicolet Avatar 320 FTIR spectrometer in the 400-4000 cm^{-1} range. ESI mass spectra were recorded on a Waters ZQ mass spectrometer using nitrogen as the drying and nebulising gas. The equipment was calibrated with appropriate standard samples. Magnetic measurements were performed with a Quantum Design MPMS-XL-5 SQUID magnetometer in the 2 to 300 K temperature range with an applied magnetic field of 0.1 T on polycrystalline samples. Mössbauer spectra were collected in transmission mode using a conventional constant-acceleration spectrometer and a 50 mCi ^{57}Co source in a Rh matrix. The velocity scale was calibrated using α-Fe foil. The absorber was obtained by gently packing single crystals of **3** into a perspex holder. Isomer shifts (Table 2) are given relative to metallic α-Fe at room temperature.

Results

Syntheses

Reaction of $Fe(ClO_4)_3 \cdot 6H_2O$, Schiff-base ligand (L_1, L_2 or L_3) and KSCN in a 1:1:2 molar ratio in methanol leads to three Fe(III) clusters with different nuclearities (8, 6 and 4) of formula $[Fe_8(\mu\text{-}L_1)_8(\mu\text{-}O)_4(NCS)_8](ClO_4)_5(NCS)_3$ (**1**), $[Fe_6(\mu\text{-}L_2)_6(\mu\text{-}O)_3(NCS)_6](ClO_4)_2(NCS)_4$ (**2**) and $[Fe_4(\mu\text{-}L_3)_2(\mu\text{-}OH)_2(\mu\text{-}OHO)(NCS)_7(OH_2)]$ (**3**), respectively. The 1:1 metal:ligand ratio of the syntheses is maintained in the final structure for compounds **1** and **2**, which contain the tetradentate imidazolyl

ligands L_1 and L_2, but not in **3**, which contains the tetradentate pyridyl ligand L_3. In this last case, the structure presents a 2:1 metal:pyridyl ligand ratio. The complexes obtained with the imidazolyl ligands are soluble in methanol and were crystallized by slow diffusion with diethyl ether. Both **1** and **2** are cationic polynuclear complexes with NCS^- and ClO_4^- acting as counterions. In contrast, similar synthetic conditions with the pyridyl-based ligand, L_3, afforded the neutral compound, **3**, which precipitated in methanol and was obtained by recrystallization in acetonitrile. The use of other counterions in the iron(III) precursor salt such as NO_3^- with L_1 and BF_4^- or Cl^- with L_2 led in all cases to hexanuclear clusters with a similar structure to that of **2** (see compounds **4** and **5,** Figs. S1 and S2, ESI†). In the case of BF_4^-, oxidation of Fe(II) to Fe(III) in air and decomposition of the anion gave rise to the presence of $[FeF_6]^{3-}$ counterions in the structure (see compound **5**, ESI). Preliminary single crystal diffraction data of a compound obtained with L_2 and Cl^- show the presence of a hexamer with a similar structure to that found in **2**, **4** and **5**. However, due to the low quality of the data it was not possible to find a proper solution of the structure. Finally, powder X-ray diffraction patterns of **2** and **3** at 300 K confirm the structure obtained from single X-ray diffraction experiments shown below (see Fig. S3, ESI†). X-ray diffraction patterns of **1** and **5** are not shown as powder samples of these compounds lost crystallinity very fast after filtering due to the loss of solvent. In the case of **4**, the small amount of sample available prevented the measurement of the powder X-ray diffraction. The composition of crystals of these compounds, checked by microanalysis, shows a Fe:S:Cl ratio close to 8:11:5 for **1**, and 6:10:2 for **2**, and a Fe:S ratio close to 4:7 for **3**, 6:6 for **4** and 6.5:10.5 for **5**.

Structure of $[Fe_8(\mu\text{-}L_1)_8(\mu\text{-}O)_4(NCS)_8](ClO_4)_5(NCS)_3(H_2O)_6$ (1)

1 crystallizes in tetragonal $I4_1cd$ space group. The structure is formed by an octanuclear cationic complex of formula $[Fe_8(\mu\text{-}L_1)_8(\mu\text{-}O)_4(NCS)_8]^{8+}$ (Fig. 1), five perchlorate and three thiocyanate anions, and disordered lattice water molecules. The octanuclear, Fe_8, unit is formed from half of the molecule, which is crystallographically independent, through a 2-fold axis linking O1 and O3. Thus, it contains four crystallographically independent Fe(III) atoms (Fe1- Fe4) and is composed by four $[Fe^{III}\text{–}O\text{–}Fe^{III}]^{4+}$ dimers. Four of the eight neutral tetradentate L_1 ligands connect the two Fe(III) of the dimer in a bis(bidentate) chelating mode while the remaining four connect Fe(III) belonging to different dimers in a similar way. Thus, each Fe(III) center shows a distorted octahedral N_5O coordination to four nitrogen atoms from two chelating L_1 in cis-arrangement, one nitrogen atom from the NCS^-, and one oxygen atom from a μ-oxo (Fig. 1). The Fe-N(imino) bond length distances range from 2.161(14) to 2.196(16) Å, while Fe-N(imidazolyl) ones range from 2.148(15) to 2.201(18) Å. In the axial position, the Fe-N(NCS^-) distances lie between 2.027(18) to 2.049(15) Å, Fe-O(oxo) are between 1.790(6) to 1.801(6) Å as normally observed for binuclear Fe(III) complexes with a single oxygen bridge.[20] These distances are in good agreement with the expected ones for high-spin (HS) Fe(III) centres. The imidazolyl NH groups in **1** present hydrogen bonds with disordered free NCS^- and ClO_4^- counterions and lattice water molecules. Two crystallographically equivalent ClO_4^- groups (with central atom Cl1) are close to the internal cavity of the Fe_8 cationic ring with numerous short contacts with L_1 atoms. On the other hand, the second crystallographically independent ClO_4^- group (with central atom Cl2) occupies the space between Fe_8 cations and present numerous short contacts with L_1 atoms.

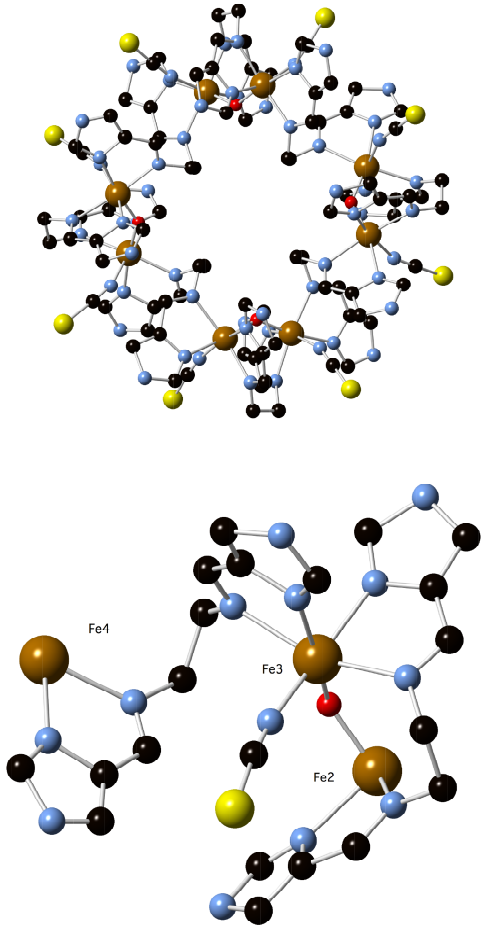

Fig. 1 Molecular structure of the octanuclear $[Fe_8(\mu\text{-}L_1)_8(\mu\text{-}O)_4(NCS)_8]^{8+}$ complex of **1** (top) and view of the coordination sphere around Fe3 linked to an iron atom from the same dimer (Fe2) and another one from the neighboring dimer (Fe4) (bottom) (iron (brown), sulfur (yellow), oxygen (red), nitrogen (blue), carbon (black)).

Structure of $[Fe_6(\mu\text{-}L_2)_6(\mu\text{-}O)_3(NCS)_6](ClO_4)_2(NCS)_4(CH_3CH_2OCH_2CH_3)_{0.5}(H_2O)_{3.5}(CH_3OH)_{2.5}$ (2)

2 crystallizes in triclinic $P\text{-}1$ space group. The structure is formed by a hexanuclear complex cation of formula $[Fe_6(\mu\text{-}L_2)_6(\mu\text{-}O)_3(NCS)_6]^{6+}$ (Fig. 2), two perchlorate and four thiocyanate anions, diethylether and disordered methanol and water molecules. The Fe_6 unit is formed by three $[Fe^{III}OFe^{III}]^{4+}$ dimers, six L_2 ligands and six NCS^- ligands. The L_2 ligands present the same intra or interdimer bis(bidentate) coordination mode

between two Fe(III) shown for compound **1**. Thus, each Fe^{III} center presents a N_5O coordination sphere to four nitrogen atoms from two chelating L_2 ligands, one nitrogen atom from the terminal NCS^- group, and one oxygen atom from an oxo group in a similar way as in compound **1**. The imidazolyl NH groups from L_2 ligands form hydrogen bonds with disordered free NCS^- counterions and lattice water and methanol molecules. The ClO_4^- groups present hydrogen bonds with the imidazolyl NH groups from L_2. One ClO_4^- group (with central atom Cl1) is very close to the internal cavity of the Fe_6 cationic ring with numerous short contacts with L_2 atoms. On the other hand, the second crystallographically independent ClO_4^- group (with central atom Cl3 with an occupancy of 0.5) is close to the opposite site of the internal cavity of the Fe_6 cationic ring. Finally, the third crystallographically independent ClO_4^- anion (with central atom Cl2 with an occupancy of 0.5) occupies the space between Fe_6 units.

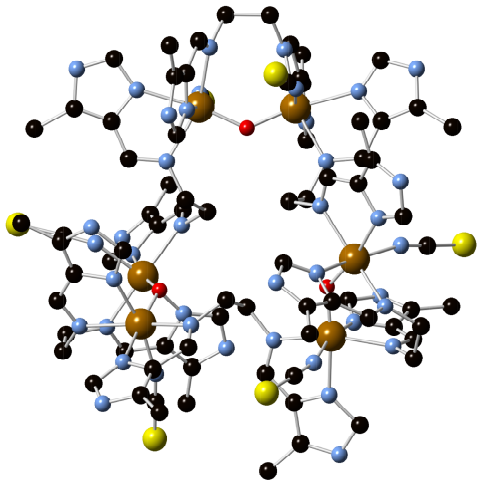

Fig. 2 Molecular structure of the hexanuclear $[Fe_6(\mu\text{-}L_2)_6(\mu\text{-}O)_3(NCS)_6]^{6+}$ complex of **2** (iron (brown), sulfur (yellow), oxygen (red), nitrogen (blue), carbon (black)).

Structure of $[Fe_4(\mu\text{-}L_3)_2(\mu\text{-}OH)_3(\mu\text{-}O)(NCS)_7(OH_2)][(H_2O)_2(CH_3CN)_{0.5}$ (3)

3 crystallizes in the monoclinic $P2_1/n$ space group. It is formed by a tetranuclear neutral complex of formula $[Fe_4(\mu\text{-}L_3)_2(\mu\text{-}OH)_3(\mu\text{-}O)(NCS)_7(OH_2)]$ and lattice water and acetonitrile solvent molecules, which are disordered in some cases. The neutral cluster is constructed from four crystallographically independent Fe(III) ions (Fe1-Fe4) that lie at the corners of a very distorted rectangle (Fig. 3). The $\mu\text{-}OH^-$ groups bridge Fe1/Fe2, Fe1/Fe3 and Fe3/Fe4 pairs (Figure 4), while Fe2/Fe4 pair is bridged by a $\mu\text{-}O^{2-}$. The Fe1/Fe3 and Fe2/Fe4 pairs are linked together by pyridyl-based L_3 ligands in bis(bidentate) chelating bridging mode. The distorted octahedral coordination of the four iron(III) ions is completed with two terminal NCS^- ligands with the exception of Fe4 which is coordinated to one terminal NCS^- ligand and one terminal water molecule (Fig. 4). Therefore, three of the four Fe(III) (Fe1, Fe2 and Fe3) present a N_4O_2 coordination sphere to two N(imine and pyridyl) from one L_3 ligand, two μ-O(hydroxo or oxo) and two N(NCS^-), while the another one (Fe4) shows a N_3O_3 coordination sphere to two N (imine and pyridyl) from one L_3 ligand, one N(NCS^-) and three μ-O(hydroxo, oxo and terminal water molecule). The four iron atoms are far to be coplanar and deviate from their best least-square plane by 0.267 (Fe1), -0.322 (Fe2), -0.286 (Fe3) and 0.341 (Fe4) Å. On the contrary, the four bridging oxygen atoms (O1 to O4) form a plane with a deviation of less than 0.006 Å from their best least-square plane.

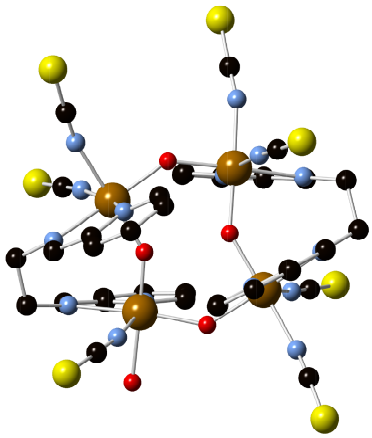

Fig. 3 Molecular structure of the tetranuclear $[Fe_4(\mu\text{-}L_3)_2(\mu\text{-}OH)_3(\mu\text{-}O)(NCS)_7(H_2O)]$ complex of **3** (iron (brown), sulfur (yellow), oxygen (red), nitrogen (blue), carbon (black)).

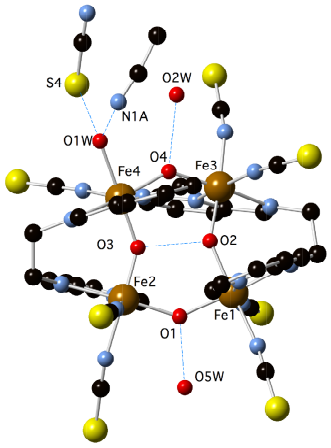

Fig. 4 Intra- and intermolecular hydrogen-bonding of **3**.

The hydrogen atoms of the Fe_4 cluster were not crystallographically located. Given the absence of counterions and the fact that metal-ligand distances and Mössbauer

spectroscopy (see below) indicate that the four metal centers are clearly HS Fe(III), charge considerations require that three of the four core oxygen are formally protonated. O1 and O4 atoms are protonated as evidenced by (i) their bond distances to Fe(III) ions (mean Fe-O distance of 1.991(3) Å), which are typical of Fe^{III}-μ-(hydroxo) bonds,[21] and (ii) the short distance of these two atoms to lattice water molecules indicating the formation of hydrogen-bonds ($d_{O1\cdots O5W}$ = 2.880 Å and $d_{O4\cdots O2W}$ = 2.780 Å). The Fe-O distances of the remaining bridging oxygens (O2 and O3) are clearly differentiated suggesting a different protonation. Thus, Fe-O distances of O2 are 1.924(3) and 1.936(3) Å, which lie in the range to that found for other Fe^{III}-μ-(hydroxo) bonds. In contrast, Fe-O distances of O3 (1.810(4) and 1.826(4) Å) are consistent with the formation of a Fe^{III}-μ-(oxo) bond (see above). Furthermore, the distance between O2 and O3 (2.551 Å) is consistent with the formation of a hydrogen bond between them (see Fig. 4). The significant difference of Fe-O distances indicating that the μ-oxo and μ-hydroxo can be considered as separate structural entities rather than a $(O\text{-}H\text{-}O)^{3-}$ unit.[22,23] Indeed, Fe_4 complexes with $(O\text{-}H\text{-}O)^{3-}$ units present shorter O···O distances ranging from 2.394 to 2.529 Å.[21,24] Finally, the presence of two protons in the terminal oxygen coordinated to Fe4 (O1W) is supported by the formation of two hydrogen bonds with one disordered lattice water/acetonitrile molecule and one S atom from a NCS^- group, as shown in Fig. 4.

Table 1. Crystallographic data for **1**, **2**, **3**, **4** and **5**

Compound	**1**	**2**	**3**
Empirical formula	$Fe_8C_{91}H_{108}N_{59}O_{30}S_{11}Cl_5$	$C_{86.5}H_{118}Cl_2Fe_6N_{46}O_{17.5}S_{10}$	$C_{36}H_{38.5}Fe_4N_{15.5}O_{7.7}S_7$
Formula weight	3484.97	2808.69	1259.26
Crystal colour	Red	Red	Red
Crystal size	0.2*0.07*0.05	0.06*0.06*0.02	0.15*0.11*0.10
Temperature (K)	120(2)	120(2)	120(2)
Wavelength (Å)	0.71073	0.71073	0.71073
Crystal system, *Z*	Tetragonal, 8	Monoclinic, 2	Monoclinic, 4
Space group	$I4_1cd$	$P\text{-}1$	$P2_1/n$
a (Å)	28.5279(3)	17.1614(6)	20.2912(6)
b (Å)	28.5279(3)	17.3252(6)	11.7876(5)
c (Å)	41.3731(6)	24.4236(7)	22.1837(6)
α (°)	90.00	70.309(3)	90
b (°)	90.00	79.499(3)	98.084(3)
γ (°)	90.00	77.344(3)	90
V (Å^3)	33671.1(9)	6624.3(4)	5253.3(3)
ρ_{calc} (Mg/m^3)	1.370	1.397	1.579
μ($Mo_{K\alpha}$) (mm^{-1})	0.960	0.910	1.422
θ range (°)	2.856-27.500	2.944-27.484	3.053-27.519
Reflns collected	178800	105489	28735
Independent reflns (R_{int})	8631 (0.1501)	14588 (0.1269)	8545 (0.0445)
L. S. parameters, *p*/ restraints, *r*	898 / 14	1479 / 7	651 / 3
$R1(F)$,[a] $I > 2\sigma(I)$	0.1109	0.0968	0.0660
$wR2(F^2)$,[b] all data	0.3470	0.3045	0.1816
$S(F^2)$,[c] all data	1.012	1.053	1.028

[a] $R1(F) = \Sigma||F_O|-|F_C||/\Sigma|F_O|$; [b] $wR2(F^2) = [\Sigma w(F_O^2-F_C^2)^2/\Sigma wF_O^4]^{1/2}$; [c] $S(F^2) = [\Sigma w(F_O^2-F_C^2)^2/(n+r-p)]^{1/2}$

Compound	**4**	**5**
Empirical formula	$C_{69}H_{86}Fe_6N_{48}O_{25}S_6$	$C_{93.5}H_{142}F_3Fe_{6.5}N_{46.5}O_{15}S_{10.5}$
Formula weight	2513.21	2914.11
Crystal colour	Red	Red
Crystal size	0.23*0.10*0.05	0.33*0.11*0.07
Temperature (K)	120(2)	120(2)
Wavelength (Å)	0.71073	0.71073
Crystal system, *Z*	Orthorhombic, 4	Monoclinic, 8
Space group	*P*bna	*C*2/c
a (Å)	15.5153(4)	45.2573(13)
b (Å)	25.8550(9)	27.5089(6)
c (Å)	26.6761(11)	28.4547(9)
α (°)	90	90
b (°)	90	119.372(4)
γ (°)	90	90
V (Å^3)	10701.1(6)	30871.7(18)
ρ_{calc} (Mg/m^3)	1.552	1.251
μ($Mo_{K\alpha}$) (mm^{-1})	0.999	0.803
θ range (°)	3.062-27.498	2.955-26.408
Reflns collected	42210	260859
Independent reflns (R_{int})	5927 (0.0934)	16529 (0.13173)
L. S. parameters, *p*/ restraints, *r*	683 / 31	1306 / 15
$R1(F)$,[a] $I > 2\sigma(I)$	0.0826	0.1149
$wR2(F^2)$,[b] all data	0.2527	0.3644
$S(F^2)$,[c] all data	1.027	1.082

[a] $R1(F) = \Sigma||F_O|-|F_C||/\Sigma|F_O|$; [b] $wR2(F^2) = [\Sigma w(F_O^2-F_C^2)^2/\Sigma wF_O^4]^{1/2}$; [c] $S(F^2) = [\Sigma w(F_O^2-F_C^2)^2/(n+r-p)]^{1/2}$

Electrospray

The behaviour of the polynuclear Fe_6 cationic cluster of **2** in solution has been characterized by electrospray ionization mass spectrometry (ESI-MS). Fig. S4., ESI,† shows the ESI-MS (positive mode) analysis of a solution of **2** in methanol. The two most intense peaks appear at m/z values of 588.67 and 598.95 Da which correspond respectively to the $[Fe_6(\mu\text{-}L_2)_6(\mu\text{-}O)_3(NCS)_6](ClO_4)(NCS)^{4+}$ and $[Fe_6(\mu\text{-}L_2)_6(\mu\text{-}O)_3(NCS)_6](ClO_4)_2^{4+}$ species. The third most intense peak corresponds to a $[Fe(L_2)(NCS)]^+$ monomer that have been reduced by one electron. Finally, the remaining peaks could be assigned to Fe_6 units that have been reduced by one electron plus one ClO_4^- (574.05 Da), one ClO_4^- and SCN^- (784.68 Da) or two ClO_4^- (798.39). The charge of the species present in the spectrum has been unambiguously characterized by single ion recording (SIR) at the highest resolution of the spectrometer with monoisotopic peaks separated by 1/z Da. Fig. S5, ESI,† shows the isotopic distributions of the most intense peaks. As the majority of peaks arise from species in which the Fe_6 core remains intact, we can conclude that the cluster is preserved in solution.

Mössbauer spectrum of 3

Owing to the structural features exhibited by the Fe_4 clusters, four different iron sites and two sorts of bridging ligands (μ-OH^- and μ-O^{2-}), it seemed to be of interest to study the Mössbauer spectrum of **3** (Fig. 5). In order to satisfactorily fit this spectrum, it was necessary to consider nested quadrupole-split doublets, i.e. of very close isomer shift (IS), in line with a very similar N_4O_2 or N_3O_3 environment for all four iron sites, but significantly different quadrupole splittings (QS). The data may in principle be analyzed assuming two quadrupole-split doublets in a 1:1 ratio with fitting parameters shown in table 2. These parameters are

typical of HS Fe(III). The quadrupole-split doublet with smaller QS value could be assigned to Fe1 and Fe3 as they exhibit very similar environments since both are linked to two μ-OH^- groups, whereas the one with larger QS could be assigned to Fe2 and Fe4, taking into account the more distorted octahedral coordination of Fe2 and Fe4 which contain shorter Fe^{III}-μ-O^{2-} bonds. Still, the Mössbauer spectrum of **3** could also be fitted to three doublets with a 2:1:1 ratio. This is not surprising given the low sensitivity of HS–Fe(III) Mössbauer parameters to the coordination environment, and the similarities of the coordination spheres of the four sites.[22] In any case and for purposes of comparison, indicative parameters of the fitting to two doublets are summarized in Table 2.

Table 2 Estimated parameters from the Mössbauer spectrum of **3** taken at room temperature.

[a]	IS	QS	Γ	I
	0.365	0.512	0.293	48.23%
	0.393	1.003	0.319	51.77%

[a] IS (mm/s) isomer shift relative to metallic Fe at 297K. QS (mm/s) quadrupole splitting of doublets; Γ (mm/s) half-width of the doublet peaks. I relative area. Estimated standard deviations are < 0.02 mm/s for IS, QS and Γ, and < 3 % for I.

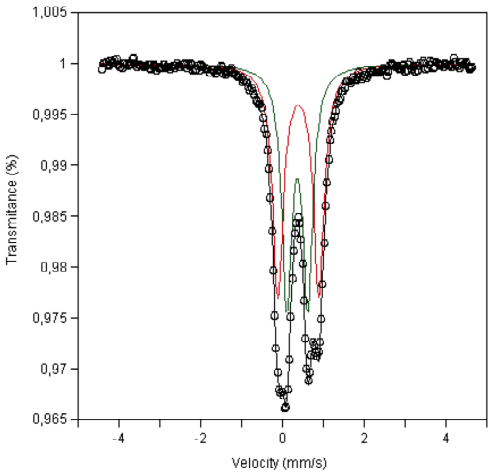

Fig. 5 Room temperature Mössbauer spectrum of **3**. The lines over the experimental points are the sum of two doublets. The estimated parameters of these doublets are collected in table 2.

Magnetic properties

The temperature dependence of the product of the molar magnetic susceptibility times the temperature (χT) of compounds **1** and **2** is shown in insets of Fig. 6. The two compounds present a very similar behaviour as expected from their structures. The χT values at 300 K (2.8 and 2.7 cm^3.K/mol for **1** and **2**, respectively) are significantly lower than theoretically expected for non-interacting HS Fe(III) ions (35.00 and 26.25 cm^3.K/mol for 8 and 6 Fe(III) ions with g=2, respectively). The χT of both compounds decreases gradually almost linearly when temperature decreases down to 50 K and stays approximately constant (0.15 cm^3.K/mol) until 2 K which is an indication of strong antiferromagnetic interactions through $[Fe^{III}–O–Fe^{III}]^{4+}$ dimer with the ground state $S = 0$. The similar χT curves of both compounds indicate that the magnetic interactions through the bis(bidentate) L_1 or L_2 ligands are very weak and that the observed behavior should be attributed to strong intradimer antiferromagnetic interactions between Fe(III) centers linked by μ-oxo. Indeed, it has been modeled using the isotropic spin-spin interaction by the Heisemberg-Dirac-Van Vleck Hamiltonian $H = -2JS_1S_2$, where $S_1 = S_2 = 5/2$.[25] To reproduce the data satisfactorily we had to consider a certain amount of a paramagnetic impurity (ρ, %). The best fit was obtained with the following parameters J = -119.2 cm-1, g= 2.00 and ρ = 0.903% for **1** (with R = 2.97×10^{-3}) and J = -110.5 cm^{-1}, g= 2.02 and ρ = 0.606% for **2** (with R = 2.82×10^{-4}). These parameters are similar to those found in other Fe^{III}-oxo dimers.[26]

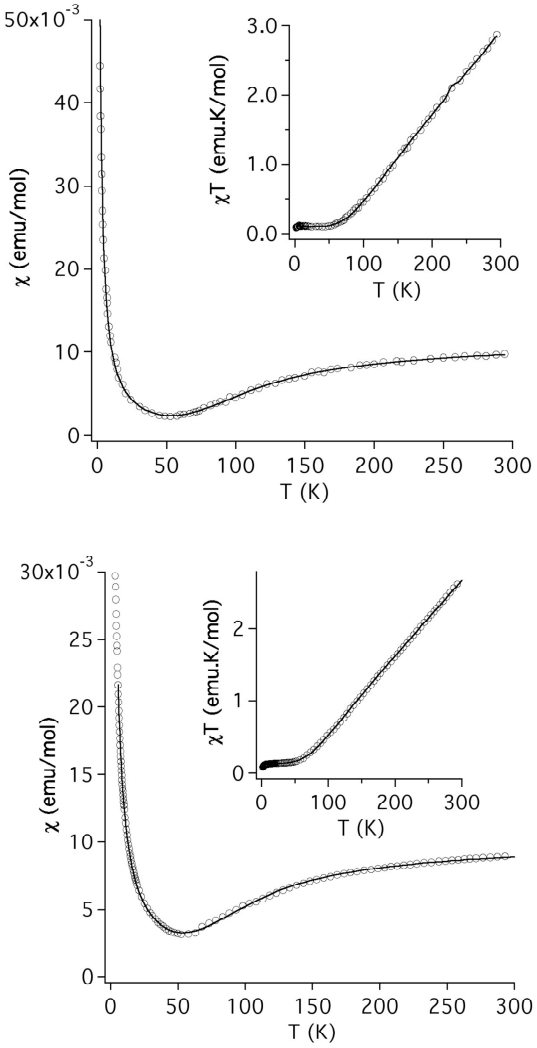

Fig. 6 Plot of χ vs T and χ_mT vs T (insets) for **1** (up) and **2** (down). The susceptibility, χ, was measured under a 0.1 T magnetic field. The solid line is the best fit of the 2-300 K data.

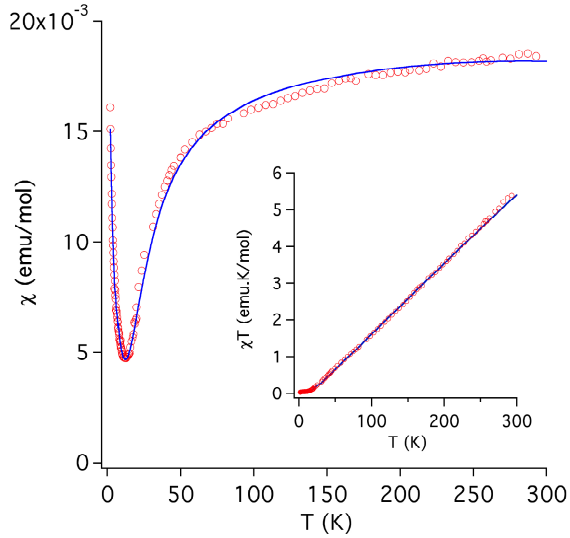

Fig. 7 Plot of χ vs T and χ_mT vs T (insets) for **3**. The susceptibility, χ, was measured under a 0.1 T magnetic field. The solid line is the best fit of the 2-300 K data.

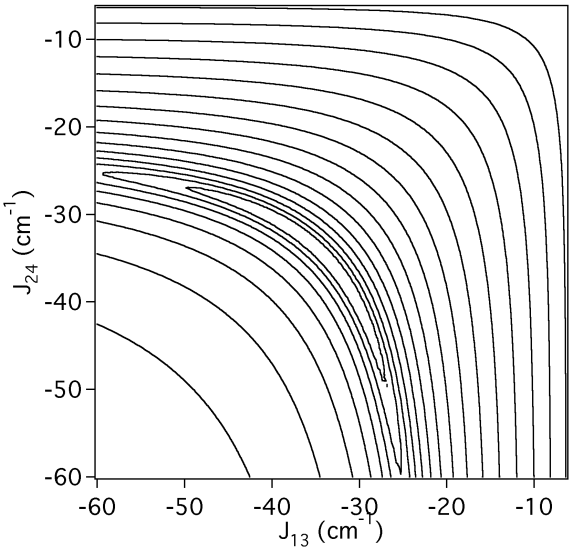

Fig. 8 Surface error plot of χ_m vs T as a function of J_{24} and J_{13} revealing a banana minima.

χT of **3** decreases linearly from 5.6 cm^3.K/mol at 300 K to 0.05 cm^3.K/mol at 10 K, and stays approximately constant down to 2 K (see inset on Fig. 7). The presence of four Fe(III) linked by μ-OH^- or μ-O^{2-} ligands gives rise to a magnetic behavior, which indicates weaker antiferromagnetic interactions between S=5/2 of the Fe(III) than those found for **1** and **2**. Inspection of the molecular structure of **3** reveals that due to the lack of symmetry, four exchange interactions would be rigorously required for the interpretation of the magnetic properties.[21] A simplification considering only three type of interactions: $J_{12} = J_{34}$ corresponding to hydroxo bridge interactions through O1 and O4 oxygen atoms, J_{13} corresponding the other type of hydroxo bridge through O2 oxygen atom and finally J_{24} associated to oxo bridge through O3 oxygen atom. The best fitting to experimental data is obtained with the following parameters $J_{12} = J_{34}$ = -3.07 cm^{-1}, $J_{24} \approx J_{13}$ = -34.37 cm^{-1}, g = 2.00 and ρ = 0.5 % (with R = 3.54×10^{-4}). This fit is not very sensible to the J_{24}/J_{13} ratio. The dependence of the fit respect to them is shown on a two-dimensional plot of the error factor R on the values J_{24} and J_{13} (See Fig. 8). The minimum error region (R < 7.0×10^{-4}) has a banana shape where both J can be interconverted and with limits at J_{13} = -27.5 cm^{-1} and J_{24} = -48.8 cm^{-1}. These parameters are similar to those found in related compounds.[21-23]

Discussion

The reactivity of iron(III) with tetradentate Schiff-base ligands derived from imidazole has been studied. In all cases the imidazolyl ligands coordinate to two iron(III) linked trough an oxo ligand in a bis(bidentate) chelating bridging mode instead of only tetradentate chelating mode observed for iron(II) systems with similar ligands. As a result of this, two novel polynuclear clusters with ring structures of eight and six iron(III) centers have been obtained in contrast to reactions of similar ligands with iron(II), which lead to mononuclear complexes in all cases. In addition, we have observed that the presence of a methyl group in the imidazolyl substituent of L_2 or the change of counterion have a drastic effect in the nuclearity of the cluster. Thus, reaction of $Fe(ClO_4)_3{\cdot}6H_2O$ with L_1 gives rise to an octanuclear iron(III) cluster, but if the size of the counteranion is reduced (replacement of ClO_4^- by NO_3^- or Cl^-) or a methyl group is introduced in the ligand (replacement of L_1 by L_2), hexanuclear clusters are obtained in compounds **2**, **4** and **5**. A possible explanation is that ClO_4^- anions present the correct size and shape to template the growth of an octanuclear cluster. Indeed, two ClO_4^- anions in the structure of compound **1** are close to the center of the octanuclear cluster and present numerous short contacts with L_1 ligands of this octanuclear cluster. When the size of the anion is reduced or bulky methyl substituents are introduced in the ligand, the octanuclear cluster cannot be formed and templating of a hexanuclear cluster occurs as in compound **4** and compound with Cl^- mentioned above with L_1 or compounds **2** and **5** with L_2. In these two last compounds, ClO_4^- or FeF_6^{3-} anions do not enter in the internal cavity of the cluster as they present short contacts with at least two neighboring hexanuclear complexes. On the other hand, replacement of the imidizolyl units by pyridyl ones leads to a tetranuclear neutral cluster of **3**, in which iron(III) is in the HS state.

ES-MS studies of methanol solutions of **2** show that the hexanuclear polynuclear complexes are preserved in solution as they form adducts with NCS^- and/or ClO_4^- counterions. This could open the way for possible applications of these clusters in solution or deposited onto surfaces.

The magnetic properties of the compounds of the octanuclear cluster of **1** and the hexanuclear cluster of **2** can be explained by the presence of four or three iron(III) dimers bridged by μ-oxo ligands that gives rise to antiferromagnetic interactions and to antiferromagnetic ground states. They could be modelled by using the isotropic spin-spin interaction with similar parameters (J = -119.2 cm-1 for **1** and J = -110.5 cm^{-1} for **2**). The angular and distance dependence of J of oxo-bridged Iron(III) dimers has been rationalized by Weihe and Güdel by using an angular and radial overlap model.[27] The similar J values of **1** and **2** are a

consequence of the similar Fe-O distances (1.790(18) Å for **1** and 1.797(5) Å for **2**) and Fe-O-Fe angles (136.7(15)º for **1** and 133.2(5)º for **2**) that they present. These values are consistent with those obtained for iron(III)-oxo dimers with similar Fe-O lengths and Fe-O-Fe angles.[27] In the case of **3**, the presence of four Fe(III) linked by μ-OH^- or μ-O^{2-} ligands gives rise to a different magnetic behavior with weaker antiferromagnetic interactions between S=5/2 of the Fe(III) than those found for **1** and **2**. The magnetic properties could be modelled by a simplified model considering only three types of interactions: $J_{12} = J_{34}$ corresponding to hydroxo bridge interactions, J_{13} corresponding the other type of hydroxo bridge and J_{24} associated to oxo. The lower value of J_{24} of **3** compared to J values of **1** and **2** is consistent with the increase of Fe-O lengths (1.818(4) Å) and Fe-O-Fe angles (145.15(18) º) for **3**.[27] As expected, the O^{2-}-bridged pair (Fe2···Fe4) is much more strongly antiferromagnetically coupled than the OH^--bridged pairs.[23] The Fe1···Fe2 and Fe3···Fe4 couplings between hydroxo-bridged pairs are similar, as expected for similarities in distances and angles. J value of these two pairs ($J_{12} = J_{34}$ = -3.07 cm^{-1}) is weaker than that of the remaining hydroxo-bridged pair (J_{13} = -27.5 cm^{-1}) as expected on the basis of the smaller Fe-O-Fe angles (~138º for Fe1-O1-Fe2 and Fe3-O4-Fe4 versus ~145º for Fe1-O2-Fe3) and longer Fe-O distances (1.993(3) Å for Fe1-O1-Fe2 and 1.990(3) Å for Fe3-O4-Fe4 versus 1.930(3) Å for Fe1-O2-Fe3).[23]

Conclusions

Two novel interesting polynuclear clusters with ring structures of eight and six Fe(III) centers have been obtained by reaction of iron(III) with tetradentate Schiff-base ligands derived from imidazole. In these compounds, the imidazolyl ligands coordinate to two Fe(III) in a bis(bidentate) chelating bridging mode instead of only tetradentate chelating mode observed for Fe(II) systems with similar ligands. In addition, the presence of a methyl group in the imidazolyl substituent or the change of counterion allows controlling the nuclearity of the cluster (from eight to six). Replacement of the imidizolyl units by pyridyl ones leads to a tetranuclear neutral cluster. This cluster presents an unusual Fe_4 structure since the presence of the L_3 ligand imposes a non-planar arrangement of the four Fe(III).

From the point of view of the magnetic properties, the presence in these clusters of pairs of HS Fe(III) ions bridged by μ-oxo or μ-hydroxo ligands gives rise to antiferromagnetic interactions and to antiferromagnetic ground states in all cases.

These results demonstrate that the reaction of iron(III) with tetradentate imidazolyl ligands is a suitable strategy to obtain new iron(III) polynuclear complexes with interesting topologies. Some small changes in the ligands such as replacement of NCS^- by CN^- could lead to a stronger ligand fields and perhaps to spin-crossover. Other interesting possibility could be the use of other metal ions with a higher magnetic axial anisotropy such as Mn(III) or lanthanides.

Acknowledgements

Financial support from the European Union (Project HINTS and ERC Advanced Grant SPINMOL), the Spanish MINECO (Project Consolider-Ingenio in Molecular Nanoscience CSD2007-00010, and projects MAT2011-22785 and CTQ-2011-26507) and the Generalitat Valenciana (Prometeo and ISIC-NANO Programs) are gratefully acknowledged. The authors thank J. M. Martínez-Agudo and Dr. G. Agustí-López, University of Valencia, for magnetic characterisation and E. Tormos, University of Valencia, for ESI-MS measurements. Manfred Womes is acknowledged for the help with Mössbauer spectroscopy.

Notes and references

[a] *Instituto de Ciencia Molecular (ICMol), Universidad de Valencia, C/ Catedrático José Beltrán 2, 46980 Paterna, Spain. Fax: 34 963543273; Tel: 34 963544419; E-mail: miguel.clemente@uv.es and eugenio.coronado@uv.es*

[b] *Materials Chemistry Research Unit, Department of Chemistry and Center of Excellence for Innovation in Chemistry, Faculty of Science, Khon Kaen University, Khon Kaen 40002, Thailand.*

† Electronic Supplementary Information (ESI) available: [ESI contain structural views of **4** and **5**, powder X-ray difftaction patterns of **2** and **3** and ES-MS of **2** in methanol]. See DOI: 10.1039/b000000x/

‡ CCDC 973767–973771 contain the supplementary crystallographic data for this paper. These data can be obtained free of charge from the Cambridge Crystallographic Data centre via www.ccdc.cam.ac.uk/data_request/cif.

1 M. D. Pluth, R. G. Bergman and K. N. Raymond, *Acc. Chem. Res.* 2009, **42**, 1650.
2 H. T. Chifotides, I. D. Giles and K. R. Dunbar, *J. Am. Chem. Soc.* 2013, **135**, 3039.
3 W. Meng, J. D. Clegg and J. R. Nitschke, *J. Am. Chem. Soc.* 2012, **51**, 1881.
4 J. M. Domínguez-Vera, A. Rodríguez, R. Cuesta, R. Kivekäs and E. Colacio, *J. Chem. Soc., Dalton Trans.* 2002, 561.
5 Y. Wang, F. –H.Zhao, A. -H. Shi, Y. -X. Che and J. -M. Zheng, *Inorg. Chem. Com.* 2012, **20**, 23.
6 J. Yao, Z. -D. Lu, Y, -Z. Li, J. -G. Lin, X. -Y. Duan, S. Gao, Q. -J. Meng and C. -S. Lu, *Cryst. Eng. Comm.* 2008, **10**, 1379.
7 (a) Z. Su, M. Chen, T. A. Okamura, M. -S. Chen, S. -S. Chen and W. -Y. Sun, *Inorg. Chem.* 2011, **50**, 985; (b) E. Coronado, M. Giménez-Marqués, G. Mínguez Espallargas and L. Brammer, *Nat. Commun.* 2012, **3**, 828.
8 (a) T. Sato, K. Nishi, S. Iijima, M. Kojima and N. Matsumoto, *Inorg. Chem.* 2009, **48**, 7211; (b) Y. Sunatsaki, R. Kawamoto, K. Fujita, H. Maruyama, T. Suzuki, H. Ishida, M. Kojima, S. Iijima and N. Matsumoto, *Coord. Chem. Rev.* 2010, **254**, 1871.
9 (a) N. Bréfuel, S. Shova, J. Lipkowski and J. -P. Tuchagues, *Chem. Mater.* 2006, **18**, 5467; (b) N. Bréfuel, I. Vang, S. Shova, F. Dahan, J. -P. Costes and J. -P. Tuchagues, *Polyhedron* 2007, **26**, 1745; (c) N. Bréfuel, S. Shova and J. -P. Tuchagues, *Eur. J. Inorg. Chem.* 2007, 4326.
10 N. Bréfuel, C. Duhayon, S. Shova and J. -P. Tuchagues, *Chem. Commun.* 2007, 5223.
11 (a) Y. Sunatsuki, Y. Ikuta, N. Matsumoto, H. Ohta, M. Kojima, S. Iijima, S. Hayami, Y. Maeda, S. Kaizaki, F. Dahan and J. -P. Tuchagues, *Angew. Chem. Int. Ed.* 2003, **42**, 1614; (b) Y. Sunatsuki, H. Ohta, M. Kojima, Y. Ikuta, Y. Goto, N. Matsumoto, S. Iijima, H. Akashi, S. Kaizaki, F. Dahan and J. -P. Tuchagues, *Inorg. Chem.* 2004, **43**, 4154; (c) N. Bréfuel, S. Imatomi, H. Torigoe, H. Hagiwara, S. Shova, J. -F. Meunier, S. Bonhommeau, J. -P. Tuchagues and N. Matsumoto, *Inorg. Chem.* 2006, **45**, 8126; (d) N. Bréfuel, H. Watanabe, L. Toupet, J. Come, N. Matsumoto, E. Collet, K. Tanaka and J. -P. Tuchagues, *Angew. Chem. Int. Ed.* 2009, **48**, 9304; (e) N. Bréfuel, E. Collet, H. Watanabe, M. Kojima, N. Matsumoto, L. Toupet, K. Tanaka and J. -P. Tuchagues, *Chem. Eur. J.* 2010, **16**, 14060.

12 R. Bagai, M. R. Daniels, K. A. Abboud and G. Christou, *Inorg. Chem.* 2008, **47**, 3318.

13 D. Gatteschi, R. Sessoli and A. Cornia, *Chem. Commun.* 2000, 725.

14 (a) X. Liu and E. C. Theil, *Acc. Chem. Res.* 2005, **38**, 167; (b) M. Faiella, C. Andreozzi, R. T. M. de Rosales, V. Pavone, O. Maglio, F. Nastri, W. F. DeGrado and A. Lombardi, *Nature Chem. Biol.* 2009, **5**, 882; (c) S. Friedle, E. Reisner and S. J. Lippard, *Chem. Soc. Rev.* 2010, **39**, 2768.

15 F. J. LaRonde and M. A. Brook, *Inorg. Chim. Acta* 1999, **296**, 208.

16 S. H. Rahaman, R. Ghosh, G. Mostafa and B. K. Ghosh, *Inorg. Chem. Commun.* 2005, **8**, 1137.

17 A. Altomare, M. C. Burla, M. Camalli, G. L. Cascarano, C. Giacovazzo, A. Guagliardi, A. G. G. Moliterni, G. Polidori and R. Spagna, *J. Appl. Cryst*. 1999, **32**, 115.

18 G. M. Sheldrick, *Acta Cryst.* 2008, **A64,** 112.

19 (a) L. J. Farrugia, *J. Appl. Cryst.* 2012, **45**, 849; (b) A.L.Spek, *J.Appl.Cryst.* 2003, **36**, 7.

20 K. Takahashi, Y. Nishida, Y. Maeda and S. Kida, *J. Chem. Soc., Dalton Trans.* 1985, 2375.

21 A. K. Singh, W. Jacob, A. K. Boudalis, J. -P. Tuchagues and R. Mukherjee, *Eur. J. Inorg. Chem*. 2008, 2820.

22 A. K. Boudalis, R. E. Aston, S. J. Smith, R. E. Mirams, M. J. Riley, G. Schenk, A. G. Blackman, L. R. Hanton and L. R. Gahan, *Dalton Trans.* 2007, 5132.

23 T. C. Stamatatos, A. G. Christou, C. M. Jones, B. J. O'Callaghan, K. A. Abboud, T. A. O'Brien and G. Christou, *J. Am. Chem. Soc.* 2007, **129**, 9840.

24 A. K. Boudalis, N. Latioti, G. A. Spyroulias, C. P. Raptopoulou, A. Terzis, V. Tangoulis and S. P. Perlepes, *J. Chem. Soc., Dalton Trans.* 2001, 955.

25 M. Scarpellini, A. Neves, A. J. Bortoluzzi, I. Vencato, V. Drago, W. A. Ortiz and C. Zucco, *J. Chem. Soc., Dalton Trans.* 2001, 2616.

26 (a) J. R. Hartman, R. L. Rardin, P. Chaudhuri, K. Pohl, K. Wieghardt, B. Nuber, J. Weiss, G. C. Papaefthymiou, R. B. Frankel and S. J. Lippard, *J. Am. Chem. Soc.* 1987, **109**, 7387; (b) U. Bossek, H. Hummel, T. Weyhermüller, E. Bill and K. Wieghardt, *Angew. Chem., Int. Ed. Engl.* 1995, **34**, 2642; (c) S. C. Payne and K. S. Hagen, *J. Am. Chem. Soc.* 2000, **122**, 6399.

27 H. Weihe and H. U. Güdel, *J. Am. Chem. Soc.* 1997, **119**, 6539.

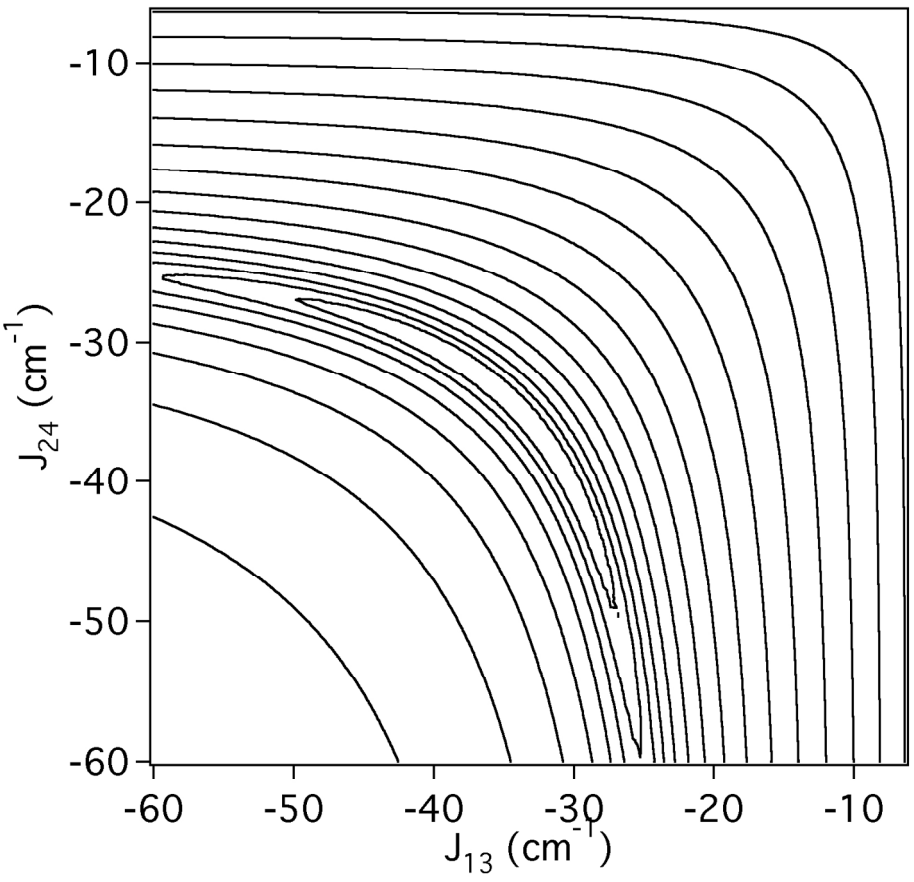

160x145mm (288 x 288 DPI)